High-fidelity simulation of a rotary bell atomizer with electrohydrodynamic effects

Venkata Krisshna*[1], Mark Owkes[2]

[1, 2]Department of Mechanical and Industrial Engineering, Montana State University, Bozeman, USA

*Corresponding author email: venkat.krisshna@gmail.com

Abstract

Rotary Bell Atomizers (RBA) are extensively used as paint applicators in the automotive industry. Atomization of paint is achieved by a bell cup rotating at speeds of 40k-60k RPM in the presence of a background electric field. Automotive paint shops amount up to 70% of the total energy costs [Galitsky et. al., 2008], 50% of the electricity demand [Leven et. al., 2001] and up to 80% of the environmental concerns [Geffen et al., 2000] in an automobile manufacturing facility. The atomization process in an RBA affects droplet size and velocity distribution which subsequently control transfer efficiency and surface finish quality. Optimal spray parameters used in industry are often obtained from expensive trial-and-error methods. In this work, three-dimensional near-cup atomization (primary and secondary breakup) are simulated computationally using a high-fidelity volume-of-fluid transport scheme that includes an electrohydrodynamic effects. The influence of fluid properties (viscosity ratio, flow rate and charge density), nozzle rotation rate and bell potential on atomization are investigated by performing a parametric study. This cost-effective method of research aims to identify the ideal spray parameters to achieve maximum transfer efficiency.

Keywords

CFD, multiphase flow, automotive painting, electric charge, NGA

Introduction

With the world becoming increasingly dependent on automotive means of transportation and motor vehicle production approaching 100 million units per year [1], automobile manufacturers are looking for ways to minimize production costs. In an automobile manufacturing facility, the paint shop can consume up to 70% of the total energy costs [2], demand up to 50% of the electricity and up to 60% of the fossil fuels or heat [3] used in the facility. This makes painting one of the most expensive processes in automobile manufacturing, consuming up to 50% of its total costs [4]. Additionally, the paint shop can account for over 80% of the environmental concerns in a manufacturing facility [5].

Rotary bell atomizers (RBAs) are extensively used as paint applicators in the automobile industry (Fig. 1a). An RBA is a high speed rotating nozzle that atomizes paint into droplets that are a few micrometers in diameter. Paint is injected onto the inner surface of a bell-shaped nozzle where it spreads into a thin film on the surface due to centrifugal forces. The high-speed rotating fluid film, on reaching the edge of the bell, exits as multiple ligaments which further atomize into droplets [6]. It is common practice to apply a background electric field and electrically charge the paint to enhance the transfer efficiency (TE) of the device [7]. Atomized droplets, which also carry electric charge, move toward the grounded target surface under the influence of the electric field.

Despite superior TE of RBAs over other paint applicators, the device is often required to overcoat the target surface to ensure sufficient finish quality [8, 9]. Owing to the impact of paint

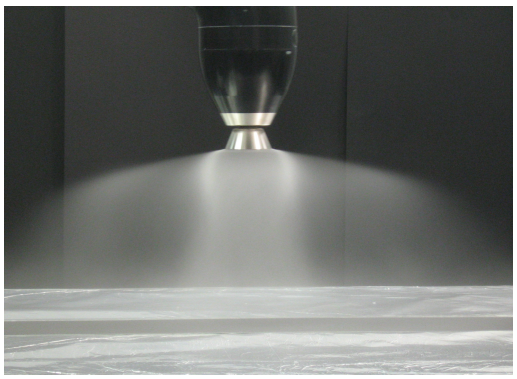

(a) A Rotary Bell Atomizer in operation. Photograph courtesy of RISE Research Institutes of Sweden and Fraunhofer-Chalmers Centre.

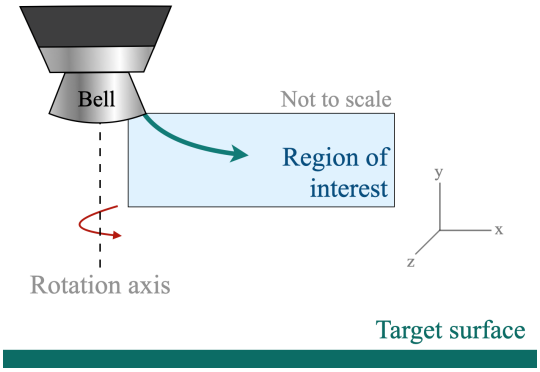

(b) Schematic of the region of interest where the physics of atomization will be studied shown in context with the bell (or the nozzle), target surface and liquid jet (teal)

shops on the operational cost of an assembly plant, it is necessary to improve the performance of RBAs to minimize costs. Metrics of significant importance such as droplet size uniformity, surface finish quality, TE, deposition thickness and the environmental impact are directly dependent on the atomization process [7, 10, 11]. Optimal nozzle operating conditions used in industry are often obtained from expensive trial-and-error experimental methods. Small improvements to the process can result in significant cost savings and waste reduction.

In addition to automobile paint shops, rotary atomizers are used in several other applications such as mass spectroscopy, agricultural spraying and air pollution control [12, 13]. Moreover, electrohydrodynamics (EHD) has seen several decades of research and is now employed in various engineering applications including inkjet printing, biochemistry and microfluidics.

Early research conducted on RBAs investigated the physics behind the atomization process in rotary atomizers [14, 15, 16, 17]. These works identified four crucial processes in the operation of RBAs - film formation, ligament formation, ligament thinning and ligament breakup [11]. Several articles have studied and characterized the process of film formation as paint flows along the bell's inner surface [18, 19] and ligament formation at the edge of the bell [20]. In this work, ligament thinning and ligament breakup are studied. Previous studies that have included an electrostatic model have explored its effects as a macroscopic phenomenon [20, 21, 22]. Generally, most prior models have given little or no attention to electric effects on multiphase transport phenomena. In this project, we aim to investigate the microscopic effects of EHD on primary and secondary atomization. Since these phenomena occur close to the bell edge in a short span of time, the domain of interest lies in a small region outside the bell (Fig. 1b).

Governing equations and methods

The methods discussed below have been implemented within a code called NGA - a high-order, fully conservative, variable density, low Mach number Navier-Stokes solver that consists of various multi-physics modules implemented in parallel using message passing interface (MPI). The formulation discretely conserves mass and momentum in a periodic domain. NGA uses a conservative unsplit geometric volume-of-fluid (VOF) scheme [23, 24, 25, 26, 27]. NGA has been developed by several groups to solve EHD flows, details of which can be found in [28, 29]. In this project, we add a physics module to account for the rotating frame which is caused by the rotating nozzle. This subjects the liquid to centrifugal and Coriolis forces which can be formulated as

$$\mathbf{f}_{\text{centrifugal}} = -\rho_i \omega \times (\omega \times r) \tag{1}$$

$$\mathbf{f}_{\text{Coriolis}} = -2\rho_i \omega \times \mathbf{u}_i \tag{2}$$

where ω is the angular velocity and r is the distance from the axis of rotation. These terms are included in Equation 2 in [29].

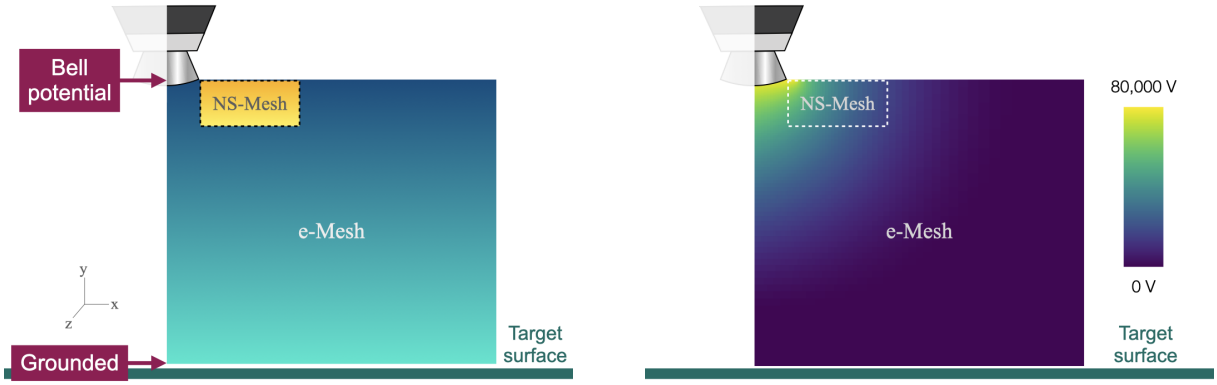

(a) e-Mesh shown in context with NS-Mesh and available ϕ BCs

(b) ϕ on e-Mesh with the location of NS-Mesh outlined with dashed lines.

Figure 2. Boundary conditions and potential field on e-Mesh (domains are not to scale)

An addition to the EHD module of NGA developed for this project involves using a domain called e-Mesh. e-Mesh is much larger than the computational domain (henceforth called the NS-Mesh) where the fluid dynamics is solved. Since our interest lies in primary and secondary atomization, NS-Mesh lies at the edge of the bell and extends a few millimeters outside it. NS-Mesh requires a well-defined potential field (ϕ) in order to obtain the electric field (**E**). We solve for ϕ using appropriate boundary conditions (BCs) at the walls of NS-Mesh. However, Fig. 2a highlights that ϕ is well defined only at the nozzle (bell potential) and at the target surface (grounded) but is not readily available at the walls of NS-Mesh. Instead of assuming values at the walls of NS-Mesh, a new domain called e-Mesh that spans between regions of well-defined ϕ is initialized and used to obtain accurate BCs on NS-Mesh. Periodic BCs are imposed on the z^+ and z^- walls of e-Mesh and Neumann BCs are imposed on its remaining walls. To make NS-Mesh as large as e-Mesh would demand computational resources to solve fluid dynamics far from the bell edge which is not of interest in this project. Thus e-Mesh is used exclusively as an electric potential solver. In addition to the BCs, e-Mesh is populated with the charge density field (q) and these are used to solve for ϕ on e-Mesh (Fig. 2b). Values of ϕ are interpolated from e-Mesh (which has a stretched grid and is coarser than NS-Mesh) to cells that lie on the walls of NS-Mesh using a tri-cubic interpolation method. These interpolated values are then used as BCs to compute ϕ on NS-Mesh.

NS-Mesh, where the fluid dynamics is solved, has dimensions of 12.96mm $\times$ 480μm $\times$ 360μm. e-Mesh, which spans from the bell edge to the target surface, has dimensions of 0.2m $\times$ 0.25m $\times$ 360μm. In RBAs, the bell edge is angled away from the axis of rotation. In the numerical setup, the jet is injected into the domain from the top wall with initial velocity components that correspond to an edge angle of 25°. The top and bottom boundaries are walls that allow slip velocity. The left boundary is a no-flux wall and the right boundary is a convective outflow. Periodic BCs are imposed on the front and back walls. The rotational axis, which is the center of the bell, is located one radial length away from the inflow at a distance of 0.025m. While many RBAs are equipped with an annular stream of focused air around the bell (called shaping air) to increase TE, the system modeled here does not include it. Since jet breakup in numerical simulations is dependent on the mesh resolution, breakup is induced by imparting velocity modulations to the inflow. The inflow velocity is modulated by adding a perturbation of 9% of itself at a superposition of three frequencies - 40 kHz, 50 kHz and 60 kHz.

Table 1. Values of simulations parameters

Property	Value	Unit
Liquid density	1000	kg/m^3
Gas density	1.204	kg/m^3
Liquid viscosity	0.1	Pa.s
Gas viscosity	1.8×10^{-5}	Pa.s
Surface tension	0.03	N/m
Bell potential	80	kV
Liquid charge density	2.879	C/m^3
Liquid relative permittivity	50	-
Gas relative permittivity	1	-
Jet inital diameter	60×10^{-6}	m
Jet initial flow rate	7.957×10^{-9}	m^3/s
Edge angle	25	degrees
Rotation rate	4×10^{4}	RPM
Bell radius	0.025	m
Diffusion constant	2×10^{-6}	m^2/s
Ionic mobility	1.79×10^{-8}	m^2/V.s

Results and discussion

Simulations are performed in a domain as described above. Table 1 contains a list of parameter values used in simulations. Fig. 3 shows the position of the liquid interface of the jet at different instances in time. We are able to capture complex and chaotic breakup activity comprising of primary and secondary atomization that occurs approximately 6mm away from the bell edge. It is to be noted that the jet contacts the bottom domain boundary after roughly 200 μs.

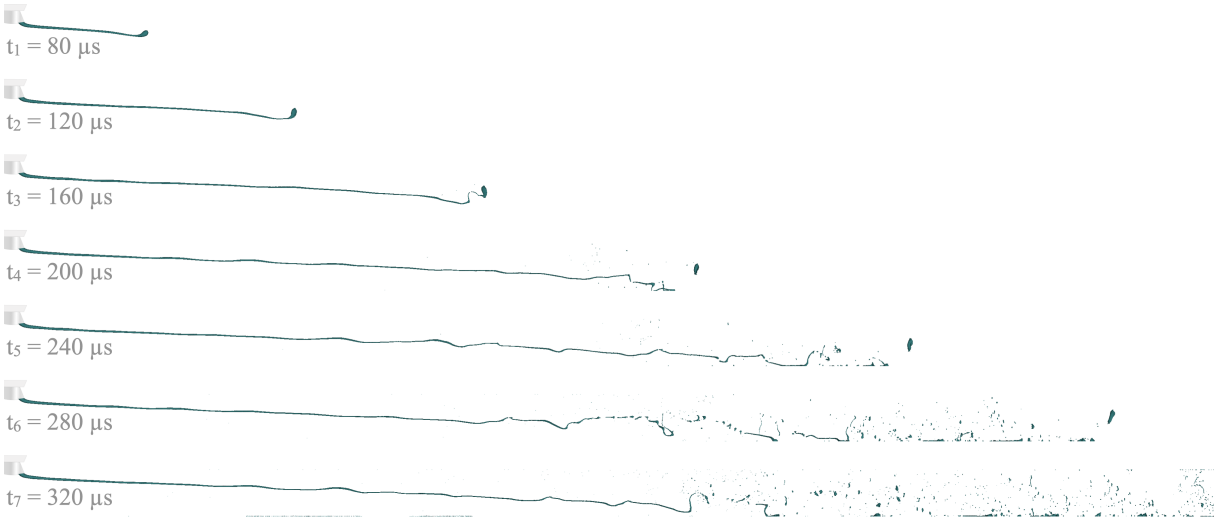

Figure 3. Liquid interface positions in the simulation at different times. The nozzle is shown for reference at the top left corner of each image and is not to scale.

An initial parameter study is performed to understand the effects of changing three operating parameters - rotation rate, flow rate and liquid viscosity - on the liquid jet. In this study, there are no EHD effects, i.e., q and ϕ are equal to 0. Results of this study are shown in Figs. 4a, 4b and 4c as snapshots of the liquid interface. The standard values of viscosity, flow rate and rotation rate are 0.1 Pa.s, 200 mL/min and 40 kRPM respectively unless otherwise stated in the figure. As the nozzle rotation rate increases, centrifugal forces are stronger on the jet and stretch it

out faster, causing early elongation and breakup. Slower rotation rates do not stretch the jet out as much in the same duration of time. A higher flow rate through the same jet diameter acts in the same way as increasing jet velocity, which initially pushes the jet out further before centrifugal forces take over. Increasing liquid viscosity delays droplet formation and ligament thinning. These results are in agreement with experimental observations [11].

Another parameter study is performed to understand the effects of EHD on the jet by changing liquid charge density q_{in} and bell potential ϕ_{bell} on the liquid jet, with standard values of 2.879 C/m^3 and 80 kV respectively. Results of the parameter study are shown in Figs. 4d and 4e as snapshots of the liquid interface. In these figures, we see that an increase in either q_{in} or ϕ_{bell} stretches the jet along its downstream direction. This is because the Coulomb force vectors point in the direction of propagation of the liquid jet. In other words, the potential field contour lines are perpendicular to velocity at that location.

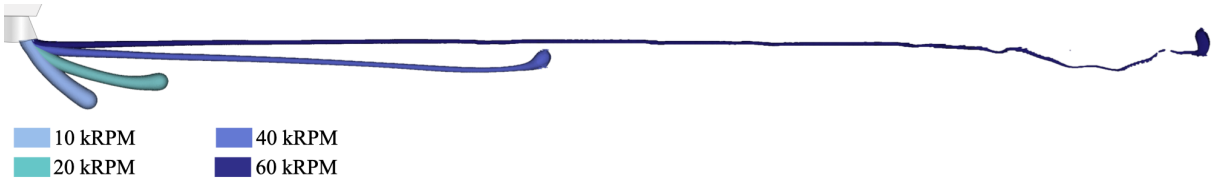

(a) Varying rotation rate, captured after 100μs

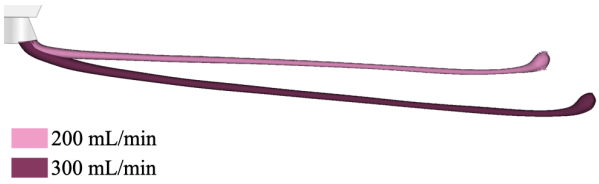

(b) Varying flow rate, captured after 100μs

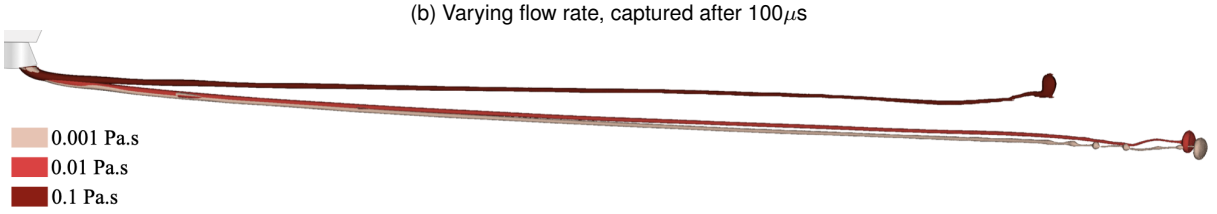

(c) Varying liquid viscosity, captured after 150μs

(d) Varying liquid charge density, captured after 150μs

(e) Varying bell potential, captured after 150μs

Figure 4. A comparison of snapshots of the liquid interface positions in the parameter study simulations. The nozzle is shown for reference at the top left corner of each image and is not to scale.

The focus of this project, however, is to investigate the effects of EHD on primary and secondary atomization. The above simulations do not provide a feasible and convenient manner of studying the physics behind EHD influenced breakup. As shown in Fig. 5, there are mainly three flow

regimes before droplet formation - 1) ligament thinning devoid of any atomization, 2) primary atomization where the jet atomizes into smaller ligaments and 3) secondary atomization where the ligaments breakup to form droplets. Here, capillary breakup is the primary phenomenon driving droplet formation. We propose a reduced physics configuration that only consists of a static perturbed ligament that undergoes capillary breakup by virtue of the Rayleigh-Plateau instability. In this reduced configuration, centrifugal and Coriolis forces are omitted. We aim to quantify the effects of a background electric field and charge repulsion on instability growth in electrically charged jets. While this has been done before both analytically and numerically by multiple research groups [30, 31, 32, 33, 34], they have often assumed an axial electric field. In RBAs, however, the Coriolis force deviates the trajectories of the jets away from the direction of the electric field. As a preliminary study, capillary breakup is simulated in a 30μm diameter ligament, results of which are shown in Fig. 6.

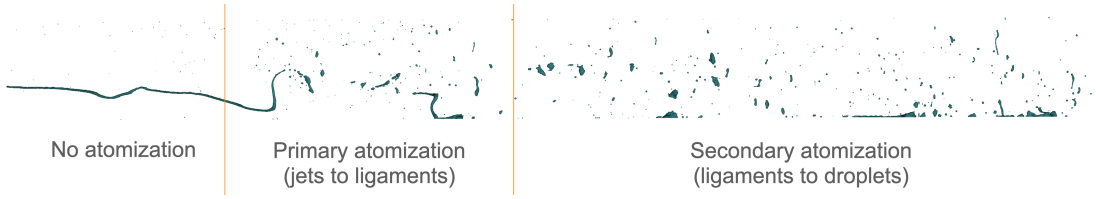

Figure 5. Different regimes of atomization in the flow. Of interest in this project is the effect of EHD on primary and secondary atomization.

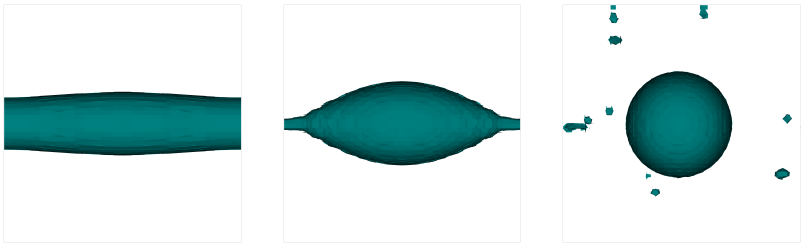

Figure 6. Capillary breakup of a 30μm diameter ligament in the absence of EHD. Periodic BCs are imposed on the left and right walls. The perturbation is sinusoidal with an amplitude that is 20% of the jet diameter across 135μm.

Conclusions

A numerical model has been developed to simulate liquid jets ejected from RBAs. The formulation includes physics modules that accurately model EHD and a rotating frame. These physics modules are built into a code called NGA. A parameter study is performed to investigate the effect of varying rotation rate, flow rate, liquid viscosity, charge density and bell potential on the jet trajectory. Observed results agree with the expected physical jet behavior and experimental results. A reduced physics configuration is proposed to further investigate the effect of EHD on primary and secondary atomization by studying its effect on capillary instability which is the primary phenomenon driving droplet formation. The effect of charge-to-mass ratio and electric field strength on instability growth and breakup will be examined using this configuration. The process of charge transport through the ligament and daughter droplets will be explored with an intent towards improving the operation of RBAs and subsequently increasing the TE.

Acknowledgements

The project is supported and funded by Ford Motor Company. The authors would like to thank Kevin Ellwood and Wanjiao Liu for their support and guidance. This material is based upon work supported by the National Science Foundation under Grant No. 1749779.

Nomenclature

ω	Angular velocity
$\mathbf{E}$	Electric field vector
ϕ	Electric potential
q	Volumetric charge density
q_{in}	Initial liquid charge density
ϕ_{bell}	Bell potential

References

[1] des Constructeurs d'Automobiles, Organisation Internationale. "World Motor Vehicle Production - 2019 Production Statistics." *International Organization of Motor Vehicle Manufacturers* .

[2] Galitsky, C. and Worrel, E. "Energy Efficiency Improvement and Cost Saving Opportunities for the Vehicle Assembly Industry: An Energy Star Guide for Energy and Plant Managers." *Lawrence Berkeley National Laboratory, University of California: Berkeley, CA, USA* .

[3] Leven, B. and Weber, C. "Energy efficiency in innovative industries: Application and benefits of energy indicators in the automobile industry." *In Proceedings ACEEE Summer Study on Energy Efficiency in Industry* Vol. 1,67-75.

[4] N. K. Akafuah, Abraham Salazar, Kimio Toda and Saito, Kozo. *Automotive Paint Spray Characterization and Visualization*. Springer Netherlands, Dordrecht (2013): pp. 121–165.

[5] Geffen, CA and Rothenberg, S. "Suppliers and environmental innovation: the automotive paint process." *International Journal of Operations and Production Management* .

[6] Frost, A. R. "Rotary atomization in the ligament formation mode." *Journal of Agricultural Engineering Research* Vol. 26 (1981): pp. 63–78.

[7] Joachim, Domnick and M., Thieme. "Atomization Characteristics of High-Speed Rotary Bell Atomizers." *Atomization and Sprays* Vol. 16 No. 8 (2006): pp. 857–874.

[8] Sadegh, Poozesh, Nelson, Akafuah and Kozo, Saito. "Effects of automotive paint spray technology on the paint transfer efficiency – a review." *Proceedings of the Institution of Mechanical Engineers, Part D: Journal of Automobile Engineering* Vol. 232 No. 2 (2018): pp. 282–301.

[9] Im, Kyoung-Su, Lai, Ming-Chia, Liu, Yi, Sankagiri, Nasy, Loch, Thomas and Nivi, Hossein. "Visualization and Measurement of Automotive Electrostatic Rotary-Bell Paint Spray Transfer Processes." *Journal of Fluids Engineering* Vol. 123 No. 2 (2000): pp. 237–245.

[10] Akafuah, Nelson K., Poozesh, Sadegh, Salaimeh, Ahmad, Patrick, Gabriela, Lawler, Kevin and Saito, Kozo. "Evolution of the Automotive Body Coating Process—A Review." *Coatings* Vol. 6 No. 2.

[11] P. L., Corbeels, Dwight W., Senser and Arthur H., Lefebvre. "Atomization Characteristics of a high speed rotary-bell paint applicator." *Atomization and Sprays* Vol. 2 No. 2 (1992): pp. 87–99.

[12] Muhammad Kashif, Iqbal Khan, Maarten, A.I. Schutyser, Karin, Schroën and Remko, Boom. "The potential of electrospraying for hydrophobic film coating on foods." *Journal of Food Engineering* Vol. 108 (2012): pp. 410–416.

[13] Ian P., Craig, Andrew, Hewitt and Howard, Terry. "Rotary atomiser design requirements for optimum pesticide application efficiency." *Crop Protection* Vol. 66 (2014): pp. 34–39.

[14] W., Balachandran and A. G., Bailey. "The Dispersion of Liquids Using Centrifugal and Electrostatic Forces." *IEEE Transactions on Industry Applications* Vol. IA-20 No. 3 (1984): pp. 682–686.

[15] Joachim, Domnick. "Effect of Bell Geometry in High-Speed Rotary Bell Atomization." 2010.

[16] Mahmoud, Ahmed and M. S., Youssef. "Influence of spinning cup and disk atomizer con-

figurations on droplet size and velocity characteristics." *Chemical Engineering Science* Vol. 107 (2014): pp. 149–157.

[17] Naoki, Igari, Takuro, Iso, Yu, Nishio, Seiichiro, Izawa and Yu, Fukunishi. "Numerical simulation of droplet-formation in rotary atomizer." *Theoretical and Applied Mechanics Letters* Vol. 9 (2019): pp. 202–205.

[18] Tatsuya, Soma, Tomoyuki, Katayama, Junichi, Tanimoto, Yasuhiro, Saito, Yohsuke, Matsushita, Hideyuki, Aoki, Daichi, Nakai, Genki, Kitamura, Masanari, Miura, Takukatsu, Asakawa, Masatoshi, Daikoku, Toshiki, Haneda, Yohsuke, Hatayama, Minori, Shirota and Takao, Inamura. "Liquid film flow on a high speed rotary bell-cup atomizer." *International Journal of Multiphase Flow* Vol. 70 (2015): pp. 96–103.

[19] Joachim, Domnick, Z., Yang and Q., Ye. "Simulation of the film formation at a high-speed rotary bell atomizer used in automotive spray painting processes." 2008.

[20] Im, Kyoung-Su, Lai, Ming-Chia, Yu, Sheng-Tao John and Matheson, Robert R. Jr. "Simulation of Spray Transfer Processes in Electrostatic Rotary Bell Sprayer ." *Journal of Fluids Engineering* Vol. 126 No. 3 (2004): pp. 449–456.

[21] Domnick, Joachim, Scheibe, Andreas and Ye, Qiaoyan. "The Simulation of the Electrostatic Spray Painting Process with High-Speed Rotary Bell Atomizers. Part I: Direct Charging." *Particle & Particle Systems Characterization* Vol. 22 No. 2 (2005): pp. 141–150.

[22] S. A., Colbert and R. A., Cairncross. "A computer simulation for predicting electrostatic spray coating patterns." *Powder Technology* Vol. 151 (2005): pp. 77–86.

[23] Guillaume, Blanquart, Perrine, Pepiot-Desjardins and Heinz, Pitsch. "Chemical mechanism for high temperature combustion of engine relevant fuels with emphasis on soot precursors." *Combustion and Flame* Vol. 156 (2009): pp. 588–607.

[24] Owkes, Mark and Desjardins, Olivier. "A mass and momentum conserving unsplit semi-Lagrangian framework for simulating multiphase flows." *Journal of Computational Physics* Vol. 332 (2017): pp. 21–46.

[25] Desjardins, Olivier, Blanquart, Guillaume, Balarac, Guillaume and Pitsch, Heinz. "High order conservative finite difference scheme for variable density low Mach number turbulent flows." *Journal of Computational Physics* Vol. 227 (2008): pp. 7125–7159.

[26] Desjardins, Olivier, Moureau, Vincent and Pitsch, Heinz. "An accurate conservative level set/ghost fluid method for simulating turbulent atomization." *Journal of Computational Physics* Vol. 227 (2008): pp. 8395–8416.

[27] Owkes, Mark and Desjardins, Olivier. "A mesh-decoupled height function method for computing interface curvature." *Journal of Computational Physics* Vol. 281 (2015): pp. 285–300.

[28] Poppel, B. P. Van, Desjardins, O. and Daily, J. W. "A ghost fluid, level set methodology for simulating multiphase electrohydrodynamic flows with application to liquid fuel injection." *Journal of Computational Physics* Vol. 229 (2010): pp. 7977–7996.

[29] Sheehy, Patrick and Owkes, Mark. "Numerical study of electric Reynolds number on electrohydrodynamic assisted atomization." *Atomization and Sprays* Vol. 27 No. 7 (2017): pp. 645–664.

[30] Melcher, J. R. "Field-Coupled Surface Waves." *Journal of Fluid Mechanics* Vol. 229 No. 4 (1963): pp. 764–764.

[31] Saville, D. A. "Stability of Electrically Charged Viscous Cylinders." *The Physics of Fluids* Vol. 14 No. 6 (1971): pp. 1095–1099.

[32] Huebner, A. L. and Chu, H. N. "Instability and breakup of charged liquid jets." *Journal of Fluid Mechanics* Vol. 49 No. 2 (1971): p. 361–372.

[33] Saville, D. A. "Electrohydrodynamic Stability: Fluid Cylinders in Longitudinal Electric Fields." *The Physics of Fluids* Vol. 13 No. 12 (1970): pp. 2987–2994.

[34] Saville, D. A. "Electrohydrodynamic stability: effects of charge relaxation at the interface of a liquid jet." *Journal of Fluid Mechanics* Vol. 48 No. 4 (1971): p. 815–827.